Talanta 240 (2022) 123196

Contents lists available at ScienceDirect

Talanta

journal homepage: www.elsevier.com/locate/talanta

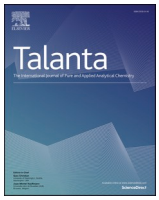

A competitive assay for the detection of a 16-mer peptide from α1 chain of human collagen XI

Ramón Lorenzo-Gómez [a,b], Alfonso Casero-Álvarez [a], Rebeca Miranda-Castro [a,b], Marcos García-Ocaña [c], Juan R. de los Toyos [b,d], Noemí de-los-Santos-Alvarez [a,b,*], M. Jesús Lobo-Castañón [a,b,**]

[a] Departamento de Química Física y Analítica. Facultad de Química, Universidad de Oviedo, Av. Julián Clavería 8, 33006, Oviedo, Spain
[b] Instituto de Investigación Sanitaria del Principado de Asturias, Av. de Roma s/n, 33011, Oviedo, Spain
[c] Unidad de Biotecnología y Ensayos Biomédicos. Servicios Científico Técnicos, Universidad de Oviedo, Oviedo, Spain
[d] Área de Inmunología, Facultad de Medicina y Ciencias de la Salud, Universidad de Oviedo, Av. Julián Clavería 6, 33006, Oviedo, Spain

ARTICLE INFO

Keywords:
Collagen XI alpha 1 chain
Aptamer
Electrochemical competitive assay
ECM component
16-Mer telopeptide
Neoepitope

ABSTRACT

Characterization of extracellular matrix (ECM) is becoming more and more important to decipher cancer progression. Constant remodeling results in ECM components degradation or unusual ECM accumulation that releases short fragments to the body fluids. These fragments might be potential cancer biomarkers but to detect them specific receptors are needed. In response to this demand, we present the first electrochemical aptamer-based competitive assay for the minor collagen XI, dysregulated in several carcinomas. It was performed on magnetic beads using enzymatic labeling. First, we selected the most appropriate tag for the aptamer (biotin or 6-carboxyfluorescein). The former yielded higher currents by chronoamperometry and it was used for the competitive assay. The collagen fragment, a 16mer peptide used as the target, was detected from 52 to 1000 nM with an RSD of about 5%. The LOD of the assay was estimated as 24 nM (44 ng/mL). The performance of the assay in serum diluted 1:2 was equivalent to the assay in PBS. The detection of α1 chain of human collagen XI was also possible in cell lysates and confirmed by aptacytofluorescence, which is promising as a new tool to validate this fragment as a cancer biomarker.

1. Introduction

The dynamic evolution of tumors requires the repetitive interrogation of patient samples usually achieved through tissue biopsies, which is not practical. For this reason, the interest in the non-invasive management of cancer has grown. In the last decade, this idea is becoming reality through the analysis of body fluids to monitor circulating components that can report about the patient's physiological state. These molecules are biomarkers. They are shed to the body fluids by not only the tumor cells but also the tumor microenvironment (TME), and its detection with this aim constitutes the diagnosis strategy named liquid biopsy [1].

There is a variety of cancer biomarkers derived from tumor cells, mainly glycoproteins with different diagnostic, prognostic and predictive value, and many others under study, but only a few have reached the clinic [2]. The clinical utility of novel tumor biomarkers such as circulating tumor cells and nucleic acids is not already fully demonstrated [3]. In the case of TME biomarkers is mostly unexplored due to their incipient postulation. The TME is composed of stromal and immune cells that are embedded in the extracellular matrix (ECM). There is an increasing body of evidence that points out to the regulatory role of ECM in several cellular processes involved in tumor growth and dissemination [4,5]. Its influence in every single cancer hallmark has been proven so that the success in cancer prevention and treatment will require the deep understanding of the interplay between tumor cells, the ECM and stromal cells [6]. To this aim, adequate probes to characterize the ECM and ascertain its contribution in tumor progression are needed [5].

* Corresponding author. Departamento de Química Física y Analítica. Facultad de Química, Universidad de Oviedo, Av. Julián Clavería 8, 33006, Oviedo, Spain.
** Corresponding author. Departamento de Química Física y Analítica. Facultad de Química, Universidad de Oviedo, Av. Julián Clavería 8, 33006, Oviedo, Spain.
E-mail addresses: lorenzoramon@uniovi.es (R. Lorenzo-Gómez), uo246417@uniovi.es (A. Casero-Álvarez), mirandarebeca@uniovi.es (R. Miranda-Castro), garciaomarcos@uniovi.es (M. García-Ocaña), jrtoyos@uniovi.es (J.R. de los Toyos), santosnoemi@uniovi.es (N. de-los-Santos-Alvarez), mjlc@uniovi.es (M.J. Lobo-Castañón).

https://doi.org/10.1016/j.talanta.2021.123196
Received 6 December 2021; Received in revised form 28 December 2021; Accepted 29 December 2021
Available online 31 December 2021

ECM is a dynamic structure essential in tissue homeostasis, so dysregulation of its components leads to pathological states [4]. The loss of ECM homeostasis implies two altered mechanisms: i) the production of collagens and other ECM proteins leading to fibrotic TME, also known as desmoplasia, and ii) ECM degradation due to overexpression of metalloproteinases. Both mechanisms cause the generation of proteolytic ECM fragments and their release into the body fluids as a protein fingerprint of the pathological state [7].

The most abundant component of the ECM is collagen, a family of closely related proteins characterized by their large size and a long triple helix core. The group of fibrillar collagens (or fibroblast-derived collagens) are synthesized as procollagens that contain N- and C- propeptides at each end. These terminal regions experience a post-translational modification by protease cleavage rendering the mature collagens that are deposited into tissues forming the interstitial ECM [8,9]. This maturation process exposes a non-helical domain hidden in the procollagen: the N- and C-telopeptides, then considered as neoepitopes.

The current marker of collagen destruction is hydroxyproline, but this molecule is not tissue specific, so it is being replaced by other compounds [10]. In the last decade, the interest in ECM fragments including those from collagens has grown because of their potential as diagnostic and prognostic biomarkers in cancer and other diseases [11–13]. Relatively large collagen fragments such as endostatin, tetrastatin, tumstatin and NC1 domain from collagen XIX are known as matrikines and present distinct biological activity from their parent intact proteins [14]. They have been found in body fluids [15–17] and their clinical utility is being studied [18–20]. Neoepitopes arisen from post-translational proteolytic breakdown of collagens lack biological activity [12] but they can be a source of biomarkers of ECM degradation/production. The clinical validity of these emerging biomarkers is still under study. Until now, neoepitopes of collagen I, II, III, IV and XI, individually or combined, have been evaluated as biomarkers in pancreatic [21–23], breast [24,25], prostate [25], hepatocellular [26] and lung [7] cancer.

Immunological techniques are the gold standard for the detection of ECM fragments. However, there are only a few antibodies specific of the neoepitopes because they are not exposed in the intact collagen. Research effort in this area is a challenge that requires mass spectrometric analysis of the metalloproteinase-cleaved fragments to find those specific of a certain collagen. Only after selecting the epitope can a probe, typically an antibody, be raised. This step is followed by the design and characterization of the immunoassay. The detection of these short fragments is commonly assessed in a competitive format with colorimetric measurements [27,28].

In order to accelerate the receptor production, to avoid the need of animals and to overcome the cross-reactivity and batch variation of antibodies, we have recently reported the development of aptamers for the C-telopeptide of the α1 chain of human collagen XI (colXIα1), a minor collagen [29]. These aptamers specifically recognize a 16-mer peptide used as the target for selection. To the best of our knowledge there is only another aptamer raised against a collagen fragment but it is a collagen I peptide [30]. The *COL11A1* gene that encodes for colXIα1 was found upregulated in tissues from patients with different carcinomas [31], especially in pancreatic ductal adenocarcinoma (PDAC), colorectal cancer [32,33] and head and neck squamous cell carcinoma [34]. It has been proposed as a specific biomarker of cancer-associated fibroblasts [35]. Until now, the only available receptors for this minor collagen were two antibodies raised against the N- and C- propeptides [23,36]. The antibody for C-propeptide was used for detection of the neoepitope in serum and showed promising prognostic value in patients with PDAC, a cancer with a very strong desmoplastic reaction [23].

In this work, we tested four candidate aptamers as receptors of 16mer peptide from colXIα1 on magnetic beads and as probes of collagen XI in cell lines. The aptamer with the highest affinity was used in an electrochemical competitive assay in complex media such as serum and cell lysates.

2. Materials and methods

2.1. Reagents

Biotin, bovine serum albumin (BSA), phosphate buffered saline 10 × concentrate, pH 7.4 (10 × PBS; 10 mM phosphate and 154 mM NaCl when diluted to 1 ×), human serum, transfer ribonucleic acid from yeast *S. cerevisiae* (tRNA), and 3,3′,5,5′-tetramethylbenzidine (TMB) liquid substrate system for ELISA, were purchased from Merck (Spain). 4′,6-Diamidino-2-phenylindole (DAPI) dihydrochloride, Dynabeads® MyOne™ Streptavidin C1, streptavidin-peroxidase conjugate (strep-POD), and Tween 20 (70%), were obtained from Thermo Fisher Scientific (Spain). 4% Formaldehyde buffered aqueous solution (pH 7) was supplied by VWR (Spain). DNA aptamers were purchased from Metabion (Germany) with a biotin or a 6-carboxyfluorescein (6FAM) tag in the 5' terminus and their sequences are shown in Table 1. Biotin-labeled 16-amino acid peptide from human collagen XI alpha 1 (16mer) was supplied by Biomedal (Spain), human recombinant vimentin (VIM) produced in *E. coli* cells was obtained from ProSpec (Israel), and human recombinant neutrophil gelatinase-associated lipocalin (NGAL) expressed in HEK cells was purchased from Abcam (United Kingdom). All DNA and protein solutions were prepared with ultrapure water and stored at appropriate concentrations at −20 °C. Water was purified with a Milli-Q system equipped with a Biopak Polisher for RNase and DNase elimination (Merck/Millipore).

2.2. Apparatus

Electrochemical measurements were performed on a μ-Autolab type II potentiostat monitored by a computer with NOVA 2.1 software (Metrohm Autolab). Screen-printed electrochemical carbon cells (SPCE, DRP-110) were supplied by Metrohm-DropSens (Spain). Each cell consisted of a carbon working electrode (4 mm of diameter), a carbon counter-electrode, and a silver pseudoreference electrode. A specific connector DRP-DSC (Metrohm-DropSens) was required to act as interface between the SPCE and the potentiostat.

Operations that required controlled temperature were performed in a ThermoMixer® Comfort (Eppendorf, Spain), while room temperature mixing steps were carried out in a Dynabeads™ MX 12-tube Mixing Wheel (Thermo Fisher Scientific). A DynaMag™-2 magnet (Thermo Fisher Scientific) was used for all the magnetic separations and washing steps.

Cell imaging experiments were performed on a confocal laser microscope TCS SP8X (Leica, Germany) provided with a PLA APO 40X/1.30 oil-immersion objective and controlled by computer with LAS X software (version 1.0.0.12269). Cell culture and staining were carried out on 4-Chamber Falcon® CultureSlides, supplied by VWR.

Table 1
DNA sequences used in this work. 6FAM and biotin-labeled anti-16mer aptamers were ordered with a 5-thymine spacer (in italics) to avoid steric hindrance in the recognition of the target. 6FAM: 6-carboxyfluorescein; FITC: fluorescein isothiocyanate.

Name	5′ label	Sequence (5' – 3′)
D1	6FAM/ Biotin	*TTT TT*G GTT GAC GGC AGT CGG TAT GCG CAT ATC GTG TTG GTA
C1	6FAM/ Biotin	*TTT TT*G GGA CTT ACT AGA GCC TGG GAG GCA AAC GCG GTA CCT GGT
G8	6FAM/ Biotin	*TTT TT*C CCG GGT ACA TTA GAA TGG TTT ACC GCC CCG CGG CGC CCT
B4	6FAM/ Biotin	*TTT TT*G ACG CAA GAA ATT CAG GGC ACC TGG AAC GAC GCG TCG GCT
Control DNA	FITC	TCT TCA CAA TAA AGT GCA AGA TAG CTG GGC AAT GGC AAA GGA TGT TAA AGG

2.3. Experimental protocols

2.3.1. Modification of streptavidin-coated magnetic beads with peptide

Dynabeads® MyOne™ Streptavidin C1 (strep-MBs) were modified according to manufacturer's indications. In brief, 50 μL of the stock solution of MBs (10 mg/mL) were pipetted on a tube and washed twice with 500 μL of 1 × PBS + 0.01% Tween 20 (washing buffer). Subsequently, 500 μL of a 2 μM solution of biotinylated 16-mer peptide prepared in 1 × PBS were added to the beads and the mixture was incubated for 30 min at 25 °C and 650 rpm. Then, the beads were washed with 500 μL of washing buffer, followed by an incubation with 500 μL of 500 μM biotin in 1 × PBS for 30 min at RT to block the remaining unoccupied streptavidin-binding sites. Finally, after washing twice with washing buffer, the 16mer-MBs were reconstituted in 500 μL of 1 × PBS (final concentration of MBs: 1 mg/mL) and stored at 4 °C until use.

2.3.2. Binding curves with peptide-modified magnetic beads

10 μL aliquots of 16mer-MBs were transferred to tubes and mixed with different concentrations of biotin-labeled aptamers in 500 μL of 1 × PBS. The mixture was incubated for 30 min at 37 °C and 650 rpm, and then the beads were washed twice with 500 μL of washing buffer. Subsequently, 500 μL of 2.5 μg/mL streptavidin-peroxidase conjugate (strep-POD) in washing buffer were added to the beads and the enzymatic labeling was performed for 30 min at RT. Next, the MBs were washed again twice with washing buffer and once with 1 × PBS and reconstituted in 15 μL of 1 × PBS. The bead solution was dropped on the working electrode of a clean carbon screen printed cell (SPCE), previously rinsed with water and ethanol and dried under a N_2 stream. The magnetic entrapment of the MBs on the surface of the working electrode was achieved with a magnet of the same size placed under it. Then, the three electrodes of the SPCE were covered with 40 μL of a commercial ready-to-use mixture of TMB and hydrogen peroxide, and the enzymatic reaction proceeded for 1 min at RT. Chronoamperometry at 0 V was carried out immediately after and the generated current was registered for 1 min.

2.3.3. Competitive assay

First, 10 μL of 16mer-MBs were transferred to a tube and mixed with a fixed amount (75 nM) of biotin-labeled D1 aptamer and increasing concentrations of 16mer peptide, in a volume of 500 μL of 1 × PBS. The mixture was incubated for 30 min at 37 °C and 650 rpm (Fig. 1, step 1). The following steps of washings, enzymatic labeling with strep-POD (Fig. 1, step 2), enzymatic reaction of TMB, and electrochemical measurement by chronoamperometry (Fig. 1, step 3), were performed as in the previous protocol. In the selectivity studies, the 16mer in solution was replaced by different proteins (BSA, vimentin or NGAL) in the first step of the assay. In experiments performed in biological media, 1 × PBS was substituted as interaction medium by 1:2 and 1:5 mixtures of serum:1 × PBS. The detection of collagen XIα1 in cell lysates was performed as usual, just by replacing 16mer in solution by the corresponding lysate. Cell lysate preparation was described previously [29]. Lysates were centrifuged prior to their use for 20 min at 4 °C and 1500 *g* to eliminate cell debris.

2.3.4. Aptacytofluorescence

Confocal microscopy imaging was performed to explore the ability of aptamers to bind to cells expressing collagen XIα1. A-204, NCI–H661 and HT-29 cell lines were obtained from the American Type Culture Collection (ATCC) and cultured according to the protocol described previously [29]. Cells were plated in the 1.7 cm^2 chambers of Falcon® CultureSlides (4×10^4 cells) and incubated for 48 h at 37 °C and 5% CO_2. After removing culture media, cells were washed for 5 min with 1 × PBS + 1 mg/mL tRNA + 1 mg/mL BSA. Subsequently, cells were incubated with 1 μM 6FAM-labeled aptamers (D1, B4 or C1) or control DNA in 1 × PBS + 0.1 mg/mL tRNA + 1 mg/mL BSA at 37 °C for 30 min. Post-incubation, cells were washed with 1 × PBS to remove unbound DNA. Then, cells were fixed with 4% formaldehyde buffered solution for 15 min at RT. After fixing, the cells were washed twice with 1 × PBS and counter-stained with 0.2 μg/mL DAPI in 1 × PBS, incubating the cells for 10 min at RT. Finally, after two washes with 1 × PBS, cells were visualized in the confocal microscope under 40X magnification. All the steps involving the use of fluorophores as well as microscopy readings were performed in the absence of light to avoid photobleaching.

3. Results and discussion

3.1. Characterization of biotinylated aptamers for 16mer binding

We have previously found several aptamers with affinity for the specific peptide of the α1 chain of human collagen XI [29]. The binding constant was estimated using aptamers labeled with 6FAM at 5' end. It is well-known that the type of label can influence the apparent K_d [37,38]. We wanted to study the effect of replacing the 6FAM by a biotin. To do this, we compared the three best aptamers (D1, C1 and G8) and we added a new one, B4, because it is the one with the strongest secondary structure ($\Delta G = -4.97$ kcal mol^{-1}) [29]. We modified strep-MBs with biotinylated 16mer peptide and, after blocking with biotin, we incubated them with increasing concentrations of each biotinylated aptamer. The amount of aptamer bound to the particles was determined by chronoamperometry after adding the strep-POD conjugate and leaving it to react with the tetramethylbenzidine (TMB) substrate. In that way, the cathodic current of TMB measured at 0 V (see the cyclic voltametric behavior of TMB in Fig. S1) is proportional to the concentration of aptamer on the surface. As expected, the current increased (in absolute terms) when the aptamer concentration increased. The binding curve (*I* vs aptamer concentration) was fitted to the Langmuir model and K_d values were estimated from the fittings (Fig. 2). D1 and B4 showed the lowest K_d values (about 170 nM), virtually identical within the

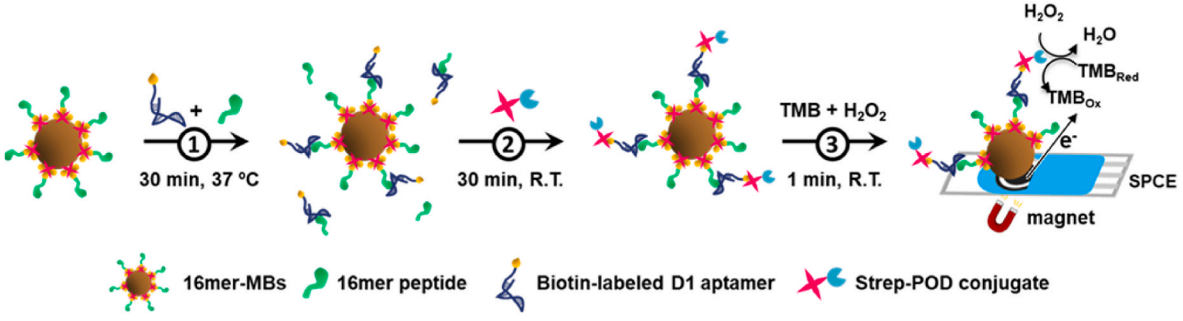

Fig. 1. Schematic depiction of the competitive assay presented in this work, which comprises the following steps: (1) Incubation of free 16mer and immobilized 16mer on strep-MBs to compete for a fixed amount of biotinylated D1 aptamer; (2) Enzymatic labeling of bound aptamer with strep-POD conjugate; (3) MBs entrapment on a screen-printed carbon cell, enzymatic reaction of TMB + H_2O_2 and electrochemical measurement by chronoamperometry.

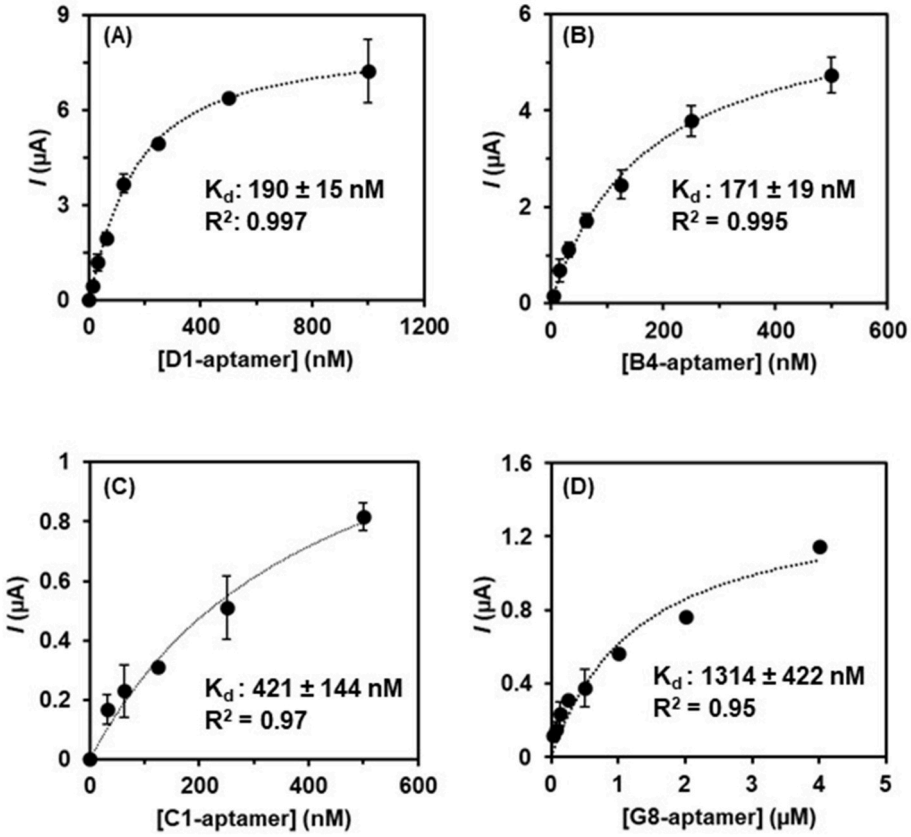

Fig. 2. Binding curves obtained on 16mer-modified strep-MBs with increasing concentration of biotinylated D1 (A), B4 (B), C1 (C) and G8 (D). The aptamer was further labeled with strep-POD and then TMB + H_2O_2 was added for 60 s. The current was measured at 0 V for 60 s by chronoamperometry. The affinity constant value (K_d) calculated by curve fitting to Langmuir model is also indicated. Error bars represent the standard deviation (n = 3).

experimental error. Both aptamers share a motif previously identified as highly prevalent in the pool of aptamers resulting from the last round of SELEX [29]. D1 has a second recurrent motif but the similarity of the K_d values indicates that the common motif [(C/G (A/C)GTCGGC] might be the most important one in the binding. C1 and G8 show a K_d of 421 nM and 1314 nM, respectively: 2.2-fold and 7.7-fold higher than D1. G8 also shows a variant of the motif carried by D1 and B4, but the level of homology is lower, which further supports its role in binding to the target.

The binding constants are lower than those measured under identical conditions with 6FAM-aptamers but the currents are much higher. For example, for D1 aptamer at 500 nM, the current with biotinylated aptamer is 6.38 μA while with 6FAM is 1.33 μA. This result is totally unexpected because streptavidin conjugate is multivalent and can bind several aptamers at a time, so the amount of conjugate is expected to be lower and so the current measured. This behavior is also observed with the rest of aptamers. Due to the high analytical signal we decided to use the biotinylated aptamers for further electrochemical experiments.

3.2. Aptacytofluorescence

To confirm the presence of collagen XI in cell lines overexpressing the protein (A-204 and NCI–H661) we used 6FAM-labeled aptamers D1, C1 and B4 to stain the cells. As negative controls we used the HT-29 cell line and an FITC-labeled unrelated DNA sequence (control DNA). Fig. 3 shows the confocal microscopy imaging of A-204, NCI–H661 and HT-29 cells treated with aptamers D1, B4 and C1 or control DNA (1 μM) and counter-stained with DAPI for nuclei visualization. Bright-field microscopy (BF) was used to enable the visualization of cell cytoplasm. BSA and tRNA were used as blocking agents to prevent aptamers from unspecifically binding to positive-charged nuclei proteins, an issue attributed to the negative charge of nucleic acid aptamers that has been widely described in literature [39–41].

Mature collagen XI alpha 1 should be located in the extracellular matrix. However, all 6FAM-labeled aptamers produced cytoplasmic fluorescent signals in A-204 cells (Fig. 3AA′, 3DD′ and 3 GG' for aptamers D1, B4 and C1, respectively). All aptamers were selected to bind a 16-amino acid peptide in the region of collagen XI alpha 1 where is expected to be enzymatically cleaved to generate the mature form, by analogy to collagen V maturation. Thus, the aptamers used in this work can bind the procollagen form, which would explain the cytoplasmic staining that we observed. On the other hand, no signal was registered in NCI–H661, even though this cell line, together with A-204, is known to express high amounts of collagen XI when cultured under induction by Transforming Growth Factor β1.

This finding could imply that under our experimental conditions, NCI–H661 cells produce less collagen XI than A-204 in agreement with our previous quantification by using commercial ELISA kits [29]. No staining was observed in the control cell line HT-29 nor in the experiments where the unrelated control DNA was used instead of aptamers.

3.3. Competitive assay

All aptamers are directed towards a small peptide. This means that it is difficult to envisage a sandwich assay due to overlapping binding sites. For this reason, a competitive assay was designed on 16mer-MBs. A fixed concentration of D1 aptamer was selected (75 nM) and incubated with increasing concentrations of 16mer in solution. The concentration of aptamer was set at 75 nM because this concentration was close to that which produces a signal about 50% of the maximum response according to the binding studies. The enzymatic labeling and the chronoamperometric measurement gave rise to a signal off assay as expected (Fig. 4A). The higher the target in solution, the lower the amount of aptamer free

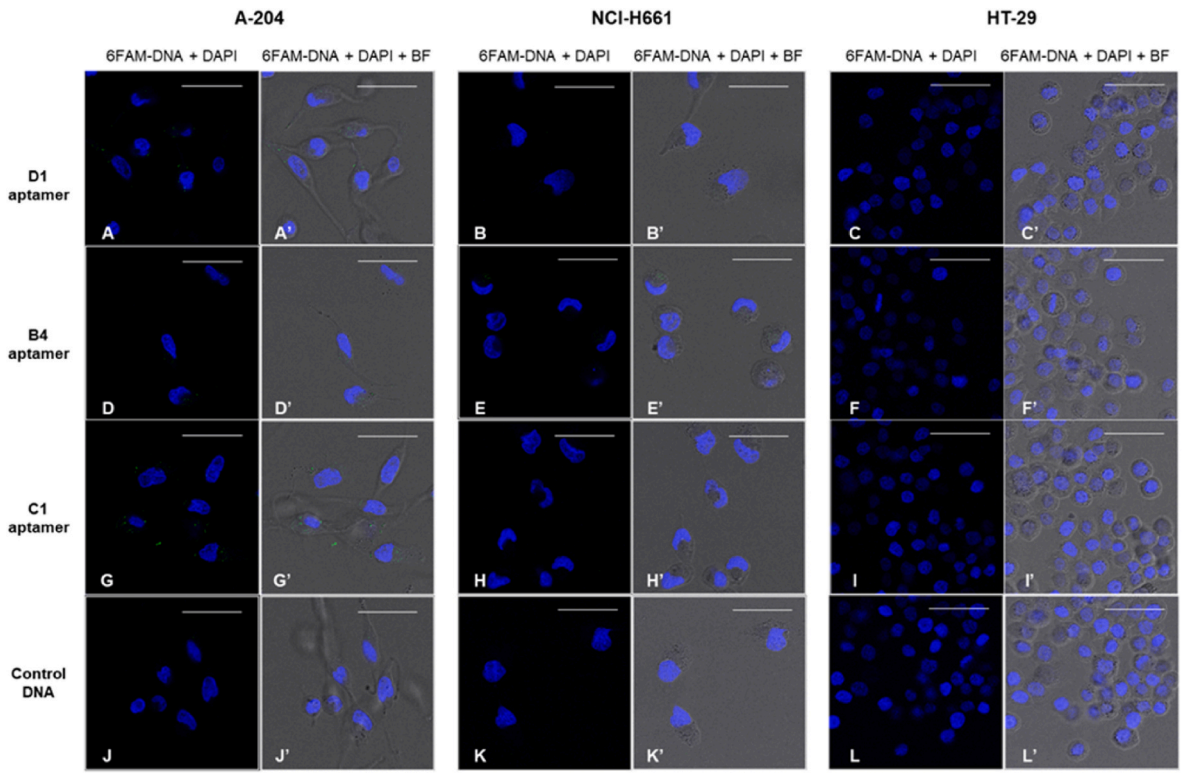

Fig. 3. Confocal microscopy imaging of cell lines A-204 (+colXIα1), NCI–H661 (+colXIα1) and HT-29 (-colXIα1) stained with 1 μM 6FAM-labeled aptamers D1 (AA′-CC′), B4 (DD′-FF′) and C1 (GG′-II′). A negative control was also performed using an unrelated fluorescein-labeled oligonucleotide (JJ′-LL′). Nuclei were counterstained with DAPI (blue) and bright field microscopy (BF) was used to help in the visualization of cells. A-L figures show merged fluorescent signals from fluorescein and DAPI while A′-L′ show fluorescent signals merged with a bright field image. Bar: 50 μm. (For interpretation of the references to color in this figure legend, the reader is referred to the Web version of this article.)

to bind the target anchored on the MBs. The *I* vs 16mer concentration plot is a sigmoidal curve that showed an excellent fitting to the 4-parameter logistic equation.

$$I\ (\mu A) = (1.28 \pm 0.04) + \frac{[(3.39 \pm 0.01) - (1.28 \pm 0.04)]}{1 + \left(\frac{0.096 \pm 0.005}{[16mer]\,(\mu M)}\right)^{(1.16 \pm 0.07)}}$$

The analytically useful interval (52–1000 nM; 95–1830 ng/mL) was defined as the concentration range comprised between the 80% and 20% of the maximum signal (no target). The LOD was estimated to be 24 nM (44 ng/mL) as the 90% of the maximum signal. The reproducibility (n = 3) at 100 nM was 5% (RSD).

The selectivity of the method was studied using several molecules. BSA was selected because it was present as blocking agent of MBs during the aptamer selection. Vimentin was tested because mass spectrometric experiments, further confirmed with electrochemical binding assays, showed that D1 aptamer is able to recognize it but with much lower affinity [29]. Lipocalin 2 or neutrophil gelatinase-associated lipocalin (NGAL) was also tested as a non-related large molecule. The competition with these molecules at 100 nM showed currents above 86% of the blank (highest current) (Fig. 4B), which indicates the aptamer hardly recognizes them. The current for the same concentration of the target was 68% of the maximum on average, showing the method is selective for the 16mer peptide.

3.4. Measurements in complex media

First, we tested the effect of using serum instead of PBS in the competitive assay. The currents in the absence and in the presence of 100 nM of 16mer when using PBS, and serum diluted 5-fold and 2-fold, are compared in Fig. 4C. The current in the absence of target was slightly higher when serum 1:5 was used. The decrease after addition of the target is similar in all three media. This result indicates that it is feasible to detect the peptide in complex media. We selected the less diluted (1:2) serum to build the competitive curve. As shown in Fig. 4A, the curve in serum is well-defined and the currents are about 24% lower than in PBS (see chronoamperograms in Fig. S2), which confirms the viability of detecting the peptide in serum without major interferences.

We also detected the collagen XI in cell lysates. With this aim, the cell lines A-204 and NCI–H661 that express the human collagen, and a negative control, the HT-29 cell line, were cultured and lysed. The lysates were centrifuged to eliminate cell debris and then incubated with 16mer-MBs in the presence of 75 nM of D1 aptamer. The currents measured by chronoamperometry (Fig. S3) were compared with that of the blank (no lysate, maximum signal) and a 100 nM of 16mer peptide (Fig. 4D). A-204 shows the largest decrease (29%) with respect to the maximum signal indicating that as expected, it is the cell line with the highest concentration of collagen XI. The collagen content of NCI–H661 cells is anticipated to be smaller than the A-204 (as observed in aptacytochemistry). Our finding indicated that indeed the concentration is smaller because the current measured is below the limit of detection of our method. The negative cell line (HT-29) shows a signal identical to the blank. As in the case of serum, there is no significant interferences from the complex media.

4. Conclusions

Monitoring the degradation or excessive production of ECM components could help the discovery of potential cancer biomarkers. We developed the first competitive assay for the detection of collagen XI α1, a potential cancer biomarker, using a novel aptamer. There are only few receptors for these hidden fragments, all of them antibodies. The

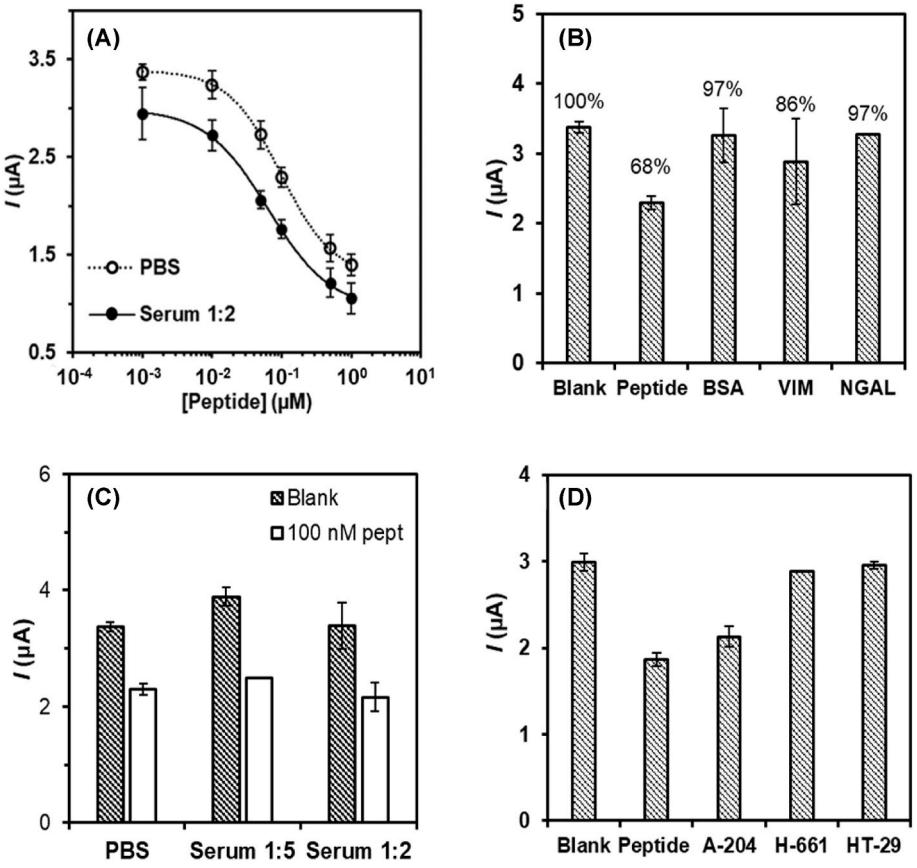

Fig. 4. (A) Electrochemical competitive assay performed on 16mer-modified strep-MBs using a fixed 75 nM concentration of D1 aptamer and increasing concentrations of 16mer in solution. The labeling and measurement steps were performed as in Fig. 1. Calibration plots obtained in 1 × PBS (white circles) and 1:2 diluted serum (black circles) are shown. (B) Selectivity assay: Currents obtained in the absence of target (blank), with BSA, vimentin (VIM), NGAL and 16mer at 100 nM with a fixed 75 nM concentration of aptamer, are shown along with the percentage of the maximum signal. (C) Performance of the competitive assay on serum: Comparison of the currents for the blank (stripped bar) and 100 nM of 16mer (white bar) in PBS, serum diluted 1:5 and 1:2. (D) Collagen XI detection in cell lysates using the competitive assay. Currents measured for the blank, the A-204, NCI–H661, HT-29 cell lines and 16mer peptide at 100 nM concentration. Measurement conditions as in Fig. 2.

aptamer-based assay was performed on magnetic beads with electrochemical detection. Two enzyme conjugates were tested and, interestingly, the multivalent streptavidin-POD showed higher currents than monovalent Fab anti-6FAM-POD. Using the former, D1 aptamer allowed the detection of collagen XIα1 fragment with a detection limit of 44 ng/mL and an analytically useful interval from 95 to 1830 ng/mL The assay proved to be selective in the presence of possible interfering proteins such us vimentin, NGAL and BSA, and showed an equivalent performance when carried out in 1:2 diluted human serum. The competitive assay was successfully challenged to detect collagen XIα1 in cell lysates. The A-204 cells overexpressing the collagen XI showed the highest response while the negative control cell line failed to show signals distinct from the blank. Aptacytofluorescence experiments with 6FAM aptamers agreed with electrochemical ones. Weak fluorescence and no electrochemical signal were observed for NCI–H661 cells, whose collagen XI expression is lower than for A-204. Together, these experiments demonstrate the ability of the aptamer to detect this target in complex samples. This competitive assay could be used to validate collagen XI as a cancer biomarker.

Credit author contribution statement

RLG: Methodology, Investigation, Data curation, Writing – original draft, Writing – review & editing. ACÁ: Investigation. RMC: Supervision, Conceptualization, Methodology, Writing – review & editing. MGO: Methodology, JRT: Conceptualization, Supervision, Writing – review & editing, NSÁ: Conceptualization, Supervision, Data curation, Methodology, Writing – original draft, Writing – review & editing. MJLC: Conceptualization, Resources, Project administration, Supervision, Writing – review & editing.

Declaration of competing interest

The authors declare that they have no known competing financial interests or personal relationships that could have appeared to influence the work reported in this paper.

Acknowledgements

This research was funded by the Spanish Government (project RTI-2018-095756-B-I00). RLG thanks the Spanish Government for a PhD fellowship (FPU16/05670). The Photonic Microscopy and Image Processing Unit from the Scientific and Technical Resources of the University of Oviedo, where confocal microscopy experiments were performed, is gratefully acknowledged.

Appendix A. Supplementary data

Supplementary data to this article can be found online at https://doi.org/10.1016/j.talanta.2021.123196.

References

[1] G. Siravegna, S. Marsoni, S. Siena, A. Bardelli, Integrating liquid biopsies into the management of cancer, Nat. Rev. Clin. Oncol. 14 (2017) 531–548, https://doi.org/10.1038/nrclinonc.2017.14.
[2] E.P. Diamandis, Cancer biomarkers: can we turn recent failures into success? J. Natl. Cancer Inst. 102 (2010) 1462–1467, https://doi.org/10.1093/jnci/djq306.
[3] G. Rossi, M. Ignatiadis, Promises and pitfalls of using liquid biopsy for precision medicine, Cancer Res. 79 (2019) 2798–2804, https://doi.org/10.1158/0008-5472.CAN-18-3402.
[4] C. Bonnans, J. Chou, Z. Werb, Remodelling the extracellular matrix in development and disease, Nat. Rev. Mol. Cell Biol. 15 (2014) 786–801, https://doi.org/10.1038/nrm3904.
[5] A. Naba, K.R. Clauser, S. Hoersch, H. Liu, S.A. Carr, R.O. Hynes, The matrisome: in silico definition and in vivo characterization by proteomics of normal and tumor

extracellular matrices, Mol. Cell. Proteomics 11 (2012), https://doi.org/10.1074/mcp.M111.014647. M111.014647.
[6] M.W. Pickup, J.K. Mouw, V.M. Weaver, The extracellular matrix modulates the hallmarks of cancer, EMBO Rep. 15 (2014) 1243–1253.
[7] N. Willumsen, C.L. Bager, D.J. Leeming, V. Smith, C. Christiansen, M.A. Karsdal, et al., Serum biomarkers reflecting specific tumor tissue remodeling processes are valuable diagnostic tools for lung cancer, Cancer Med 3 (2014) 1136–1145, https://doi.org/10.1002/cam4.303.
[8] H.P. Bächinger, K. Mizuno, J.A. Vranka, S.P. Boudko, Collagen formation and structure, in: H.-W. Liu, L. Mander (Eds.), Comprehensive Natural Products II, Elsevier, Oxford, 2010, pp. 469–530, https://doi.org/10.1002/cam4.303.
[9] S. Ricard-Blum, The collagen family, Cold Spring Harbor Perspect. Biol. 3 (2011) a004978, https://doi.org/10.1101/cshperspect.a004978.
[10] H.W. Woitge, M.J. Seibel, Markers of bone and cartilage turnover, Exp. Clin. Endocrinol. Diabetes 125 (2017) 454–469, https://doi.org/10.1055/s-0043-106438.
[11] N.I. Nissen, M. Karsdal, N. Willumsen, Collagens and cancer associated fibroblasts in the reactive stroma and its relation to cancer biology, J. Exp. Clin. Cancer Res. 38 (2019) 115, https://doi.org/10.1186/s13046-019-1110-6.
[12] S. Ricard-Blum, S.D. Vallet, Fragments generated upon extracellular matrix remodeling: biological regulators and potential drugs, Matrix Biol. 75–76 (2019) 170–189, https://doi.org/10.1016/j.matbio.2017.11.005.
[13] R. Lorenzo-Gómez, R. Miranda-Castro, N. de-los-Santos-Álvarez, M.J. Lobo-Castañón, Bioanalytical methods for circulating extracellular matrix-related proteins: new opportunities in cancer diagnosis, Anal. Bioanal. Chem. (2021), https://doi.org/10.1007/s00216-021-03416-2.
[14] J.C. Monboisse, J.B. Oudart, L. Ramont, S. Brassart-Pasco, F.X. Maquart, Matrikines from basement membrane collagens: a new anti-cancer strategy, Biochim. Biophys. Acta 1840 (2014) 2589–2598, https://doi.org/10.1016/j.bbagen.2013.12.029.
[15] A. Dupont-Deshorgue, J.B. Oudart, B. Brassart, G. Deslee, J.M. Perotin, M. D. Diebold, et al., A competitive enzyme-linked immunosorbent assay for quantification of tetrastatin in body fluids and tumor extracts, Anal. Biochem. 482 (2015) 16–21, https://doi.org/10.1016/j.ab.2015.04.023.
[16] J.B. Oudart, S. Brassart-Pasco, E. Luczka, A. Dupont-Deshorgue, G. Bellon, S. P. Boudko, et al., Analytical methods for measuring collagen XIX in human cell cultures, tissue extracts, and biological fluids, Anal. Biochem. 437 (2013) 111–117, https://doi.org/10.1016/j.ab.2013.03.007.
[17] Y.-Q. Luo, L.-J. Yao, L. Zhao, A.-Y. Sun, H. Dong, J.-P. Du, et al., Development of an ELISA for quantification of tumstatin in serum samples and tissue extracts of patients with lung carcinoma, Clin. Chim. Acta 411 (2010) 510–515, https://doi.org/10.1016/j.cca.2010.01.001.
[18] Z.-H. Wang, Z.-T. Zhu, X.-Y. Xiao, J. Sun, Correlation of serum levels of endostatin with tumor stage in gastric cancer: a systematic review and meta-analysis, BioMed Res. Int. 2015 (2015) 623939, https://doi.org/10.1155/2015/623939.
[19] T. Szarvas, V. László, F. vom Dorp, H. Reis, A. Szendröi, I. Romics, et al., Serum endostatin levels correlate with enhanced extracellular matrix degradation and poor patients' prognosis in bladder cancer, Int. J. Cancer 130 (2012) 2922–2929, https://doi.org/10.1002/ijc.26343.
[20] S.H. Nielsen, N. Willumsen, S. Brix, S. Sun, T. Manon-Jensen, M. Karsdal, et al., Tumstatin, a matrikine derived from collagen Type IVα3, is elevated in serum from patients with non–small cell lung cancer, Transl Oncol 11 (2018) 528–534, https://doi.org/10.1016/j.tranon.2018.02.005.
[21] N. Willumsen, C.L. Bager, D.J. Leeming, V. Smith, M.A. Karsdal, D. Dornan, et al., Extracellular matrix specific protein fingerprints measured in serum can separate pancreatic cancer patients from healthy controls, BMC Cancer 13 (2013) 554, https://doi.org/10.1186/1471-2407-13-554.
[22] N. Willumsen, S.M. Ali, K. Leitzel, J.J. Drabick, N. Yee, H.V. Polimera, et al., Collagen fragments quantified in serum as measures of desmoplasia associate with survival outcome in patients with advanced pancreatic cancer, Sci. Rep. 9 (2019) 19761, https://doi.org/10.1038/s41598-019-56268-3.
[23] N.I. Nissen, S. Kehlet, A.Z. Johansen, I.M. Chen, M. Karsdal, J.S. Johansen, et al., Noninvasive prognostic biomarker potential of quantifying the propeptides of Type XI collagen alpha-1 chain (PRO-C11) in patients with pancreatic ductal adenocarcinoma, Int. J. Cancer 149 (2021) 228–238, https://doi.org/10.1002/ijc.33551.
[24] A. Lipton, K. Leitzel, S.M. Ali, H.V. Polimera, V. Nagabhairu, E. Marks, et al., High turnover of extracellular matrix reflected by specific protein fragments measured in serum is associated with poor outcomes in two metastatic breast cancer cohorts, Int. J. Cancer 143 (2018) 3027–3034, https://doi.org/10.1002/ijc.31627.
[25] D.J. Leeming, M. Koizumi, P. Qvist, V. Barkholt, C. Zhang, K. Henriksen, et al., Serum N-terminal propeptide of collagen type I is associated with the number of bone metastases in breast and prostate xancer and xorrelates to other bone related markers, Biomarkers Cancer 3 (2011) 15–23, https://doi.org/10.4137/BIC.S6484.
[26] C. Jensen, S. Holm Nielsen, M. Eslam, F. Genovese, D.J. Leeming, M.J. Nielsen, et al., Cross-linked multimeric pro-peptides of type III collagen (PC3X) in hepatocellular carcinoma - a biomarker that provides additional prognostic value in AFP positive patients, J. Hepatocell. Carcinoma 7 (2020) 301–313, https://doi.org/10.2147/JHC.S275008.
[27] A.-C. Bay-Jensen, Q. Liu, I. Byrjalsen, Y. Li, J. Wang, C. Pedersen, et al., Enzyme-linked immunosorbent assay (ELISAs) for metalloproteinase derived type II collagen neoepitope, CIIM—increased serum CIIM in subjects with severe radiographic osteoarthritis, Clin. Biochem. 44 (2011) 423–429, https://doi.org/10.1016/j.clinbiochem.2011.01.001.
[28] D.J. Leeming, Y. He, S.S. Veidal, Q.H.T. Nguyen, D.V. Larsen, M. Koizumi, et al., A novel marker for assessment of liver matrix remodeling: an enzyme-linked immunosorbent assay (ELISA) detecting a MMP generated type I collagen neo-epitope (C1M), Biomarkers 16 (2011) 616–628, https://doi.org/10.3109/1354750X.2011.620628.
[29] R. Lorenzo-Gómez, R. Miranda-Castro, J.R. de los Toyos, N. de-los-Santos-Álvarez, M.J. Lobo-Castañón, Aptamers targeting a tumor-associated ECM component: the human mature collagen XIα1, Anal. Chim. Acta 1189 (2022) 339206, https://doi.org/10.1016/j.aca.2021.339206.
[30] J.G. Bruno, M.P. Carrillo, T. Phillips, D. Hanson, J.A. Bohmann, DNA aptamer beacon assay for C-telopeptide and handheld fluorometer to monitor bone resorption, J. Fluoresc. 21 (2011) 2021, https://doi.org/10.1007/s10895-011-0903-6.
[31] Z. Raglow, S.M. Thomas, Tumor matrix protein collagen XIα1 in cancer, Cancer Lett. 357 (2015) 448–453, https://doi.org/10.1016/j.canlet.2014.12.011.
[32] H. Fischer, R. Stenling, C. Rubio, A. Lindblom, Colorectal carcinogenesis is associated with stromal expression of COL11A1 and COL5A2, Carcinogenesis 22 (2001) 875–878, https://doi.org/10.1093/carcin/22.6.875.
[33] J.A. Galván, J. García-Martínez, F. Vázquez-Villa, M. García-Ocaña, C. García-Pravia, P. Menéndez-Rodríguez, et al., Validation of COL11A1/procollagen 11A1 expression in TGF-β1-activated immortalised human mesenchymal cells and in stromal cells of human colon adenocarcinoma, BMC Cancer 14 (2014) 867, https://doi.org/10.1186/1471-2407-14-867.
[34] J.C. Sok, J.A. Lee, S. Dasari, S. Joyce, S.C. Contrucci, A.M. Egloff, et al., Collagen type XI α1 facilitates head and neck squamous cell cancer growth and invasion, Br. J. Cancer 109 (2013) 3049–3056, https://doi.org/10.1038/bjc.2013.624.
[35] C. García-Pravia, J.A. Galván, N. Gutiérrez-Corral, L. Solar-García, E. García-Pérez, M. García-Ocaña, et al., Overexpression of COL11A1 by cancer-associated fibroblasts: clinical relevance of a stromal marker in pancreatic cancer, PLoS One 8 (2013), e78327, https://doi.org/10.1371/journal.pone.0078327.
[36] M. García-Ocaña, F. Vázquez, C. García-Pravia, N. Fuentes-Martínez, P. Menéndez-Rodríguez, F. Fresno-Forcelledo, et al., Characterization of a novel mouse monoclonal antibody, clone 1E8.33, highly specific for human procollagen 11A1, a tumor-associated stromal component, Int. J. Oncol. 40 (2012) 1447–1454, https://doi.org/10.3892/ijo.2012.1360.
[37] E. González-Fernández, N. de-los-Santos-Álvarez, A.J. Miranda-Ordieres, M. J. Lobo-Castañón, Monovalent labeling system improves the sensitivity of aptamer-based inhibition assays for small molecule detection, Sensor. Actuator. B Chem. 182 (2013) 668–674, https://doi.org/10.1016/j.snb.2013.03.070.
[38] R. Lorenzo-Gómez, N. Fernández-Alonso, R. Miranda-Castro, N. de-los-Santos-Álvarez, M.J. Lobo-Castañón, Unravelling the lipocalin 2 interaction with aptamers: may rolling circle amplification improve their functional affinity? Talanta 197 (2019) 406–412, https://doi.org/10.1016/j.talanta.2019.01.057.
[39] S. Gupta, D. Thirstrup, T.C. Jarvis, D.J. Schneider, S.K. Wilcox, J. Carter, et al., Rapid histochemistry using slow off-rate modified aptamers with anionic competition, Appl. Immunohistochem. Mol. Morphol. 19 (2011) 273–278, https://doi.org/10.1097/PAI.0b013e3182008c29.
[40] Z. Zhao, L. Xu, X. Shi, W. Tan, X. Fang, D. Shangguan, Recognition of subtype non-small cell lung cancer by DNA aptamers selected from living cells, Analyst 134 (2009) 1808–1814, https://doi.org/10.1039/b904476k.
[41] M. Bauer, J. Macdonald, J. Henri, W. Duan, S. Shigdar, The application of aptamers for immunohistochemistry, Nucleic Acid Therapeut. 26 (2016) 120–126, https://doi.org/10.1089/nat.2015.0569.